Journal of Cluster Science (2023) 34:2509–2519
https://doi.org/10.1007/s10876-022-02402-7

ORIGINAL PAPER

# Fenton-like Cerium Metal–Organic Frameworks (Ce-MOFs) for Catalytic Oxidation of Olefins, Alcohol, and Dyes Degradation

**Walid Sharmoukh**[1] · **Hani Nasser Abdelhamid**[2,3,4]

Received: 31 August 2022 / Accepted: 2 December 2022 / Published online: 2 January 2023


## Abstract

A metal–organic framework (MOF) of cerium (Ce) ions and 4,4′,4″-nitrilotribenzoic acid linker was synthesized via a hydrothermal method. Ce-MOF consists of a Lewis acid moiety, i.e. $Ce^{3+}$ and triphenylamine cores. It showed Fenton-like properties with excellent catalytic oxidation activity for olefins, primary/secondary alcohols, and water pollutants e.g., organic dyes. It displayed high oxidation conversion of cinnamyl alcohol and styrene of 100% and 53%, respectively. It offered good selectivity towards styrene oxide and benzaldehyde (i.e. 75% and 100%, respectively). It was applied for the oxidative degradation of dyes e.g. rhodamine B (RhB), methyl blue (MeB), Congo red (CR), and direct blue (DB) using hydrogen peroxide ($H_2O_2$) as an oxidant. It exhibited high efficiency in the oxidative degradation of these water pollutants. The mechanistic study of oxidation involves the formation of radical hydroxyl ($^{\bullet}OH$) species. This study revealed the possibility of enhancing the oxidative catalytic performance, including oxidative degradation of organic pollutants, by employing advanced oxidation processes (AOPs) using Ce-MOF. The catalyst is recyclable five times without significantly decreasing of the material's catalytic performance.

**Keywords** MOFs · Cerium-based MOFs · Oxidation · Alcohol oxidation · Dye degradation

## Introduction

The catalysis process involves over 80% of industrial processes representing annual global sales of $1.5 trillion (equal to 35% of the world's Gross domestic product (GDP) [1]. Among several catalytic reactions, the oxidation of organic molecules such as alkenes/olefins, alcohol, and dyes is essential for environmental concerns and the synthesis of fine chemicals such as pharmaceuticals, paints, and surfactants. The conversion of alcohols via oxidation reaction to aldehydes is critical for the organic synthesis of industrial and valuable molecules. Furthermore, the catalytic oxidation reaction is necessary for several applications, such as the oxidation of air pollutants [2, 3], volatile organic compounds (VOCs) [4–7], and aqueous pollutants for water treatment [8–10]. Thus, the ongoing research focuses on developing an appropriate catalyst for the oxidation reaction. The typical synthesis procedure of carbonyl compounds (e.g., aldehydes and ketones) uses a high amount of oxidizing agents such as potassium permanganate. However, these oxidants caused environmentally unfriendly residues. Thus, further exploration should be taken to find a suitable oxidant with low environmental negative impact. The noble metal was reported to catalyze the alcohol oxidation for fine-chemistry applications [11–13]. They exhibit high catalytic activity with excellent selectivity. However, they are expensive and require precaution during application or recycling.

With the increase in world population, there is an exponential rise in the demand for clean drinking water [14]. Fenton and Fenton-like reaction using nanomaterials advanced catalytic oxidation of organic pollutants for

✉ Hani Nasser Abdelhamid
hany.abdelhamid@aun.edu.eg; hani.nasser@bue.edu.eg

1 Department of Inorganic Chemistry, National Research Centre, Advanced Materials Technology and Mineral Resources Research Institute, El Tahrir St, Dokki, Giza 12622, Egypt

2 Advanced Multifunctional Materials Laboratory, Department of Chemistry, Faculty of Science, Assiut University, Assiut 71516, Egypt

3 Proteomics Laboratory for Clinical Research and Materials Science, Department of Chemistry, Assiut University, Assiut, Egypt

4 Nanotechnology Research Centre (NTRC), The British University in Egypt (BUE), Suez Desert Road, El-Sherouk City, Cairo 11837, Egypt

degradation and water treatment [10, 15]. These reactions are called advanced oxidation processes (AOPs) [16]. The reaction generates highly oxygen reactive species (ROS) or hydroxyl radicals ($^{\bullet}OH$) via the reaction between a catalyst and $H_2O_2$. Several catalysts were reported for AOPs [10]. Explore new materials may advance AOPs for high catalytic performance and better selectivity toward the target molecules [17].

Metal–organic frameworks (MOFs) display attractive properties including high surface area, tunable pores, chemical structure, and increased activity as heterogeneous catalysts [18–26]. They can be applied to several trends, such as energy, environmental, and biomedical [27, 28]. MOFs advanced water treatment and remediation [29]. They can exhibit nanozyme activity and serve as Fenton and Fenton-like materials [30]. Among several MOFs categories, cerium-based MOFs are promising for further exploration as catalysts [31]. Ce-based MOFs showed higher Fenton-like efficiency than other iron-based heterogeneous catalysts [32]. They offer good nanozyme activity. However, there are few reported examples in the literature. It was reported that cerium oxide is a practical support for alcohol oxidation compared to other supports such as carbon, $TiO_2$, and $Fe_2O_3$ [33].

Herein, the present work describes the rational construction of Ce-MOF based on 4,4′,4″-nitrilotribenzoic acid ($H_3NTB$), and $Ce^{3+}$ ion [28, 34]. Ce-MOF was examined for the catalytic oxidation of olefins and alcohol (primary and secondary) using peroxides as oxidants. We investigated the use of different peroxides, such as tert-butyl hydrogen peroxide (TBHP, t-BuOOH), benzoyl peroxide (PhCOOOH), and hydrogen peroxide ($H_2O_2$). Ce-MOF was also investigated for dye removal via the oxidative degradation of methylene blue (MB), Congo Red (CR), Rhodamine 6G (Rh6G), and direct blue (DB). Data analysis suggests that Ce-MOF is a promising catalyst for the oxidation reaction of olefins, alcohol, and organic pollutants.

## Materials and Experimental

### Materials

Cerium nitrate hexahydrate, MB, CR, Rh6G, DB, TBHP, benzoyl peroxide (PhCOOOH), and hydrogen peroxide ($H_2O_2$), benzyl alcohol, acetonitrile (AC), dichloromethane, N-hexane, dimethylformamide (DMF), and ethyl acetate were purchased from Sigma-Aldrich (Germany). $H_3NTB$ was synthesized following the procedure of Ref. [28]

### Synthesis of Ce-MOF

Ce-MOF was synthesized via a hydrothermal method using $Ce^{3+}$ salt (0.14 g) and $H_3NTB$ (0.12 g) [27, 28]. The reactants were dissolved in a solvent mixture of DMF, $H_2O$, and HCl (0.1 M) with a ratio of 10: 1: 2 (vol: vol) via ultrasonication. The reaction mixture was kept at 85 °C for 16 h. The product was soaked in methanol for 24 h before washing further with ethanol (2 × 25 mL).

### Oxidation of Olefins and Alcohol

Typical reactions of olefins oxidation included oxidants such as anhydrous tert-butyl hydroperoxide (0.32 mL, 1.92 mmol) in decane, catalyst (0.08 mol.% metal sites), and substrate such as styrene (0.19 g, 1.9 mmol). A two-necked flask (25 mL) is connected to a condenser for catalytic oxidation using an oil bath and a nitrogen atmosphere. We purged the solution three times with $N_2$ to remove the dissolved gases. After that, the reactants were stirred for 10 h at 75 °C. The completeness of the reaction was confirmed via gas chromatography-mass spectrometry (GC–MS), thin-layer chromatography (TLC), and proton nuclear magnetic resonance ($^1$H NMR).

For the recycling experiment, the catalyst after recovery was used for the subsequent reaction without being rinsed with ethanol or evacuated. The catalytic reactions were measured three times, and the results were collected and analyzed to emphasize the catalytic results' reproducibility.

The effect of catalyst loading was investigated using 5–100 mg mass weight. Typically, alcohol (benzyl alcohol, 0.20 g, 1.8 mmol), water (1 mL), and Ce-MOF (5, 10, 50, 100 mg) were used following the same procedure shown above procedure using stirring at 50 °C, and $H_2O_2$ (0.38 g, 0.33 mL, 11.09 mmol). The reaction was followed using TLC (eluent of EtOAc: cyclohexane, a ratio of 2:10 (vol: vol)).

The conversion and selectivity were calculated using $^1$H NMR spectra. They can be calculated using the following equations:-

$$\text{Conversion of alcohol} = \frac{\int \textit{Proton Signals of The Product}}{\int \textit{Proton Signals for Reactants}}$$

$$\text{Selectivity(S)} = \frac{\int \textit{Proton Signals of each Product}}{\int \textit{Total Proton Signals of the Products}}$$

After the complete reactions, the products were separated via extraction using dichloromethane. The extract was characterized using GC–MS.

### Catalytic Oxidative Degradation of Organic Pollutants

Stock solutions of the organic dyes (i.e. MB, Rh6G, DB, and CR, 10 mg) were dissolved in 10 mL of deionized water. 10 mg of Ce-MOF and 5 mL $H_2O_2$ (30 wt.%) were added to the solution. The reaction was followed via withdrawing 10 µL of the dye's solution. The sample was diluted using water to 3 mL for measuring using a UV–Vis spectrophotometer.

### Characterization Instruments

Phillips 1700 X'Pert using Cu $K_\alpha$ X-ray radiation was used to record X-ray diffraction (XRD). Oxidation state and chemical composition were measured using X-ray photoelectron spectra (XPS, Thermo Fisher, K-alpha). Fourier transform infrared spectroscopy (FT-IR) was recorded via a Nicolet spectrophotometer model 6700. The proton ($^1$H) and carbon ($^{13}$C) analyses were evaluated on Bruker 400 MHz instruments using $CDCl_3$ or DMSO-d6. UV–Vis spectra were measured using a spectrophotometer (Agilent Cary Eclipse). GC–MS spectra of the reaction crude were recorded using Shimadzu 2014 (Japan). The analyte was separated using a column equipped with ShinCarbon ST micropacked (Restek, USA) and detected via mass spectrometry. The temperatures of the mass spectrometry (MS) transfer line and Ion source were 280 °C and 300 °C, respectively. The photoluminescence emission spectra for terephthalic acid and hydrogen peroxide with and without Ce-MOF were evaluated via Cary Eclipse (Agilent, USA) using an excitation wavelength of 315 nm.

## Result and Discussion

### Materials Characterization

Solvothermal synthesis of Ce-MOF involves coordinating $Ce^{3+}$ ions and $H_3$NTB (Fig. 1a). XRD (Fig. 1b), FT-IR (Fig. 1c), and XPS (Fig. 1d) were reported for the material characterization. XRD pattern reveals that Ce-MOF has high crystallinity (Fig. 1b). There is a sharp peak below Bragg

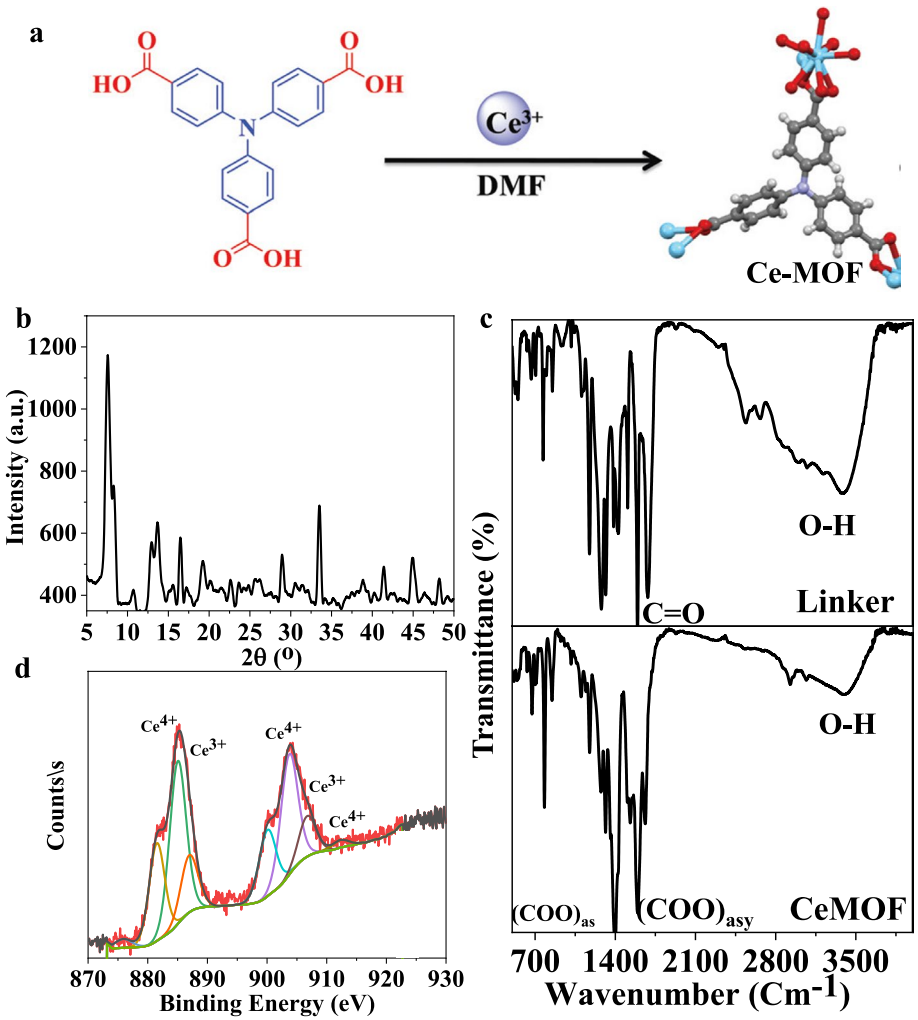


**Fig. 1** **a** the synthesis procedure of Ce-MOF and **b–d** characterization of Ce-MOF using **b** XRD, **c** FT-IR, and **d** XPS

**Scheme 1** Oxidation of olefins and alcohols using Ce-MOF as catalyst and peroxide as oxidant

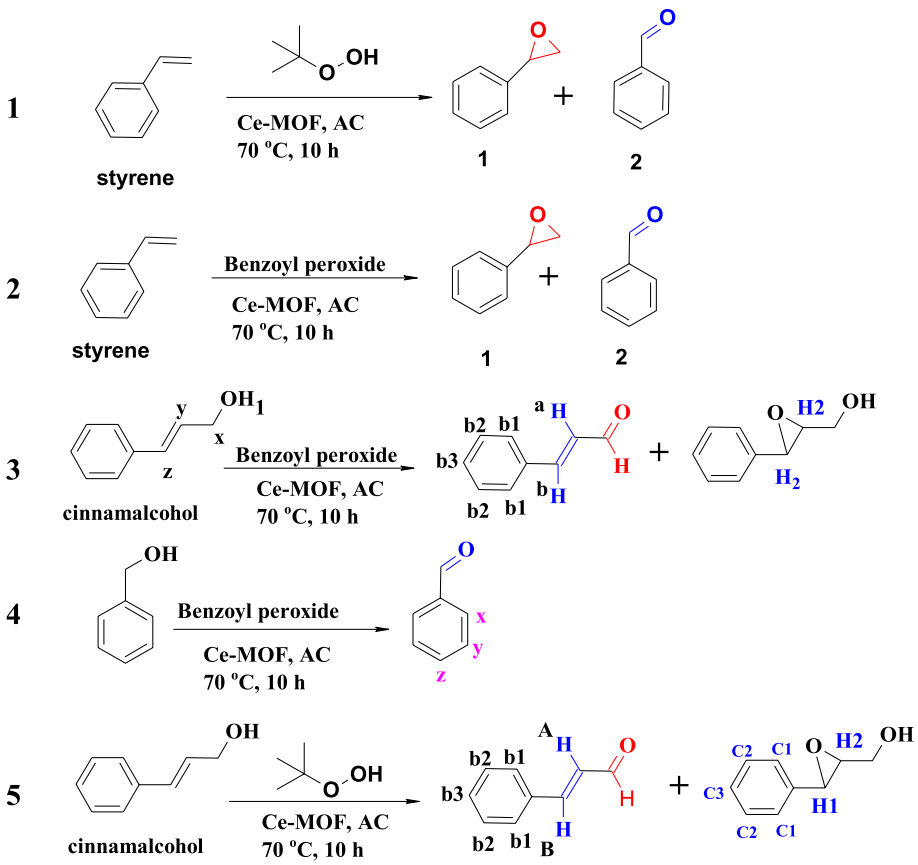


angle 10°, meaning the formation of a large unit cell of Ce-MOF, i.e. the construction of a coordination polymer. The FT-IR spectra ensured the bonds between $Ce^{3+}$ ions and $H_3NTB$ (Fig. 1c). $H_3NTB$ displayed a strong vibrational peak for the C = O bond at 1690 $cm^{-1}$ (Fig. 1c) [35–38]. It showed bands at 1595 $cm^{-1}$ and 1410 $cm^{-1}$ after coordination with cerium clusters, corresponding to asymmetric and symmetric stretching of coordinated carboxylate ($COO^-$) ions, respectively [39, 40]. The oxidation state of cerium was evaluated using XPS analysis (Fig. 1d). XPS spectrum of Ce 3d displayed mixed oxidation states of $Ce^{3+}$ and $Ce^{4+}$ with a weight ratio of 6% ($Ce^{4+}/Ce^{3+}$, Fig. 1d) [41, 42].

## Catalytic Oxidation of Alcohols and Olefins

Ce-MOF was tested for the oxidation of alcohol and olefins using styrene, benzyl alcohol, and cinnamyl alcohol as model substrates. The Ce clusters in Ce-MOF are coordinated with water molecules, allowing accessible Lewis and Brønsted acid sites [34, 43]. Thus, it can be used as efficient catalytic oxidation. Olefins oxidation was reported for styrene as a model using Ce-MOF and peroxide as catalyst and oxidant, respectively (Scheme 1). The reaction was evaluated using $^1H$ NMR for the crude reaction (Fig. 2). $^1H$ NMR spectrum shows the signal of both reactants and products (Fig. 2). Using tert-butyl peroxide as an oxidant, the optimum conditions resulted in styrene oxide and benzaldehyde forming. In Table 1, Ce-MOF demonstrated a conversion of styrene of 45% with high selectivity toward styrene oxide (75%) over benzaldehyde (25%). Using benzoyl peroxide as an oxidant, Ce-MOF produced a moderate transformation of styrene to benzaldehyde (70%) and styrene oxide (30%).

The product of styrene oxidation is further confirmed using GC–MS (Fig. 3a-b). Mass spectrometry (MS) spectra confirm the presence of styrene oxide and benzaldehyde with a residual of the reactant, i.e. styrene. MS spectra show peaks at *m/z* of 104, 106, and 120, corresponding to styrene, benzaldehyde, and styrene oxide, respectively (Fig. 3**c**). The observed peaks at *m/z* 105, 91, and 77 are assigned to phenyl carbonyl ions ($PhCO^+$, $C_7H_5CO^+$), tropylium ions ($PhCH_2^+$, $C_7H_7^+$), and phenyl ($Ph^+$, $C_6H_5^+$), respectively (Fig. 3**c**). GC–MS analysis confirms styrene's oxidation to styrene oxide and benzaldehyde (Fig. 3). The conversion was also calculated using GC–MS. Data analysis confirms conversion of 99.5% with the selectivity of 20% and 80% for benzaldehyde and styrene oxide, respectively. GC–MS analysis confirm the data obtained from $^1H$ NMR. Ce-MOF offers two main advantages: the short reaction time and the high selectivity toward epoxidation over the formation of benzaldehyde.

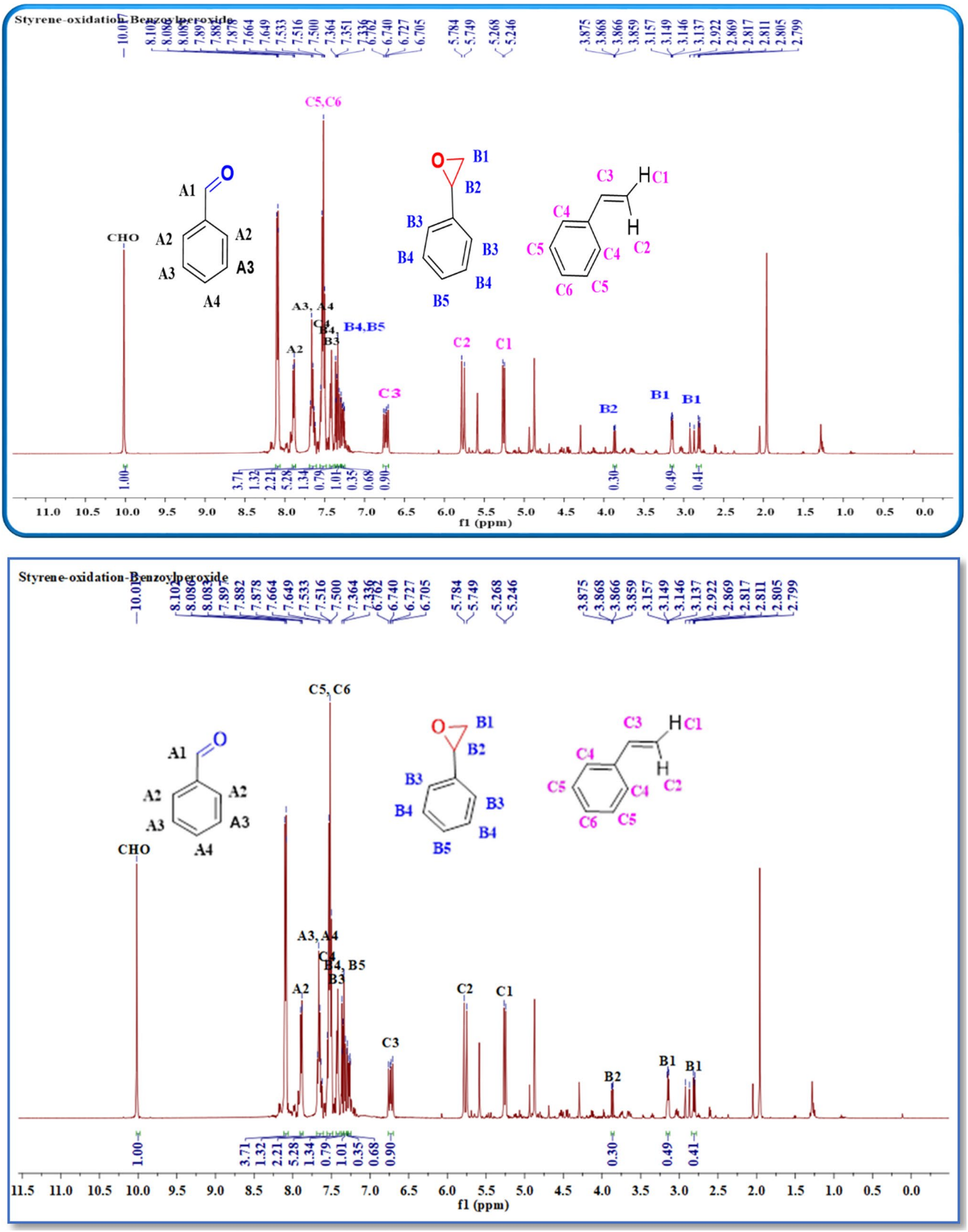


**Fig. 2** $^{1}$H NMR for styrene oxidation using Ce-MOF as a catalyst; Styrene (1.8 mmol), water (1 mL), and Ce-MOF (100 mg), stirring at 50 °C, and $H_2O_2$ (11.09 mmol)

**Table 1** Oxidation of styrene using Ce-MOF and peroxides

| Entry | Reagent | Conversion% | Selectivity% | |
|---|---|---|---|---|
| | | | 1 | 2 |
| 1 | tert-Butyl hydroperoxide | 45 | 75 | 25 |
| 2 | Benzoyl peroxide | 53 | 30 | 70 |
| 3 | Benzoyl peroxide | 15 | 56 | 44 |
| 4 | Benzoyl peroxide | 30 | 100 | |
| 5 | tert-Butyl hydroperoxide | 100 | 47 | 53 |

Alcohol (1.8 mmol), water (1 mL), and Ce-MOF (100 mg), stirring at 50 °C, and $H_2O_2$ (11.09 mmol)

We investigate the oxidation of alcohol using benzyl alcohol and cinnamyl alcohol as models using Ce-MOF and two oxidants, i.e. benzoyl peroxide and tert-butyl peroxide (Scheme 1). The oxidation of cinnamyl alcohol using benzoyl peroxide offers low conversion (15%) with high selectivity toward cinnamaldehyde and (3-phenyl oxiran-2-yl)methanol of 56% and 44%, respectively. In contrast, the oxidation of cinnamyl alcohol using tert-butyl peroxide resulted in high conversion and selectivity of 47% and 53%, respectively (Table 1).

Nine MOFs based on Ce-based UiO-66 were reported by combining two different linker molecules in sizes and functionalities. The Ce-UiO-66-benzene-1,4-dicarboxylic (BDC)/TEMPO (2,2,6,6-tetramethylpiperidine-1-oxyl radical) catalyzed the aerobic oxidation of benzyl alcohol, offering a conversion of 88% [47]. Au/MOF-5 offered 66% and 3% conversion for methyl benzoate and benzaldehyde, respectively, using benzyl alcohol in a basic pH medium. It showed that 69% conversion was observed without base, resulting in 33% methyl benzoate. Au/Al-MIL-53 (Materials of Institute Lavoisier, MIL) showed a 98% oxidation benzyl alcohol, offering a selectivity of 2% and 77% for benzaldehyde and methyl benzoate, respectively [48]. However, an optimal sub-stoichiometric amount of tert-butyl peroxide, $H_2O_2$, or benzoyl peroxide enable aerobic oxidation of benzyl alcohol with an excellent selectivity of 100%. Ce-MOF promotes the benzyl alcohol oxidation in acetonitrile at 70 °C when combined with sodium carbonate,

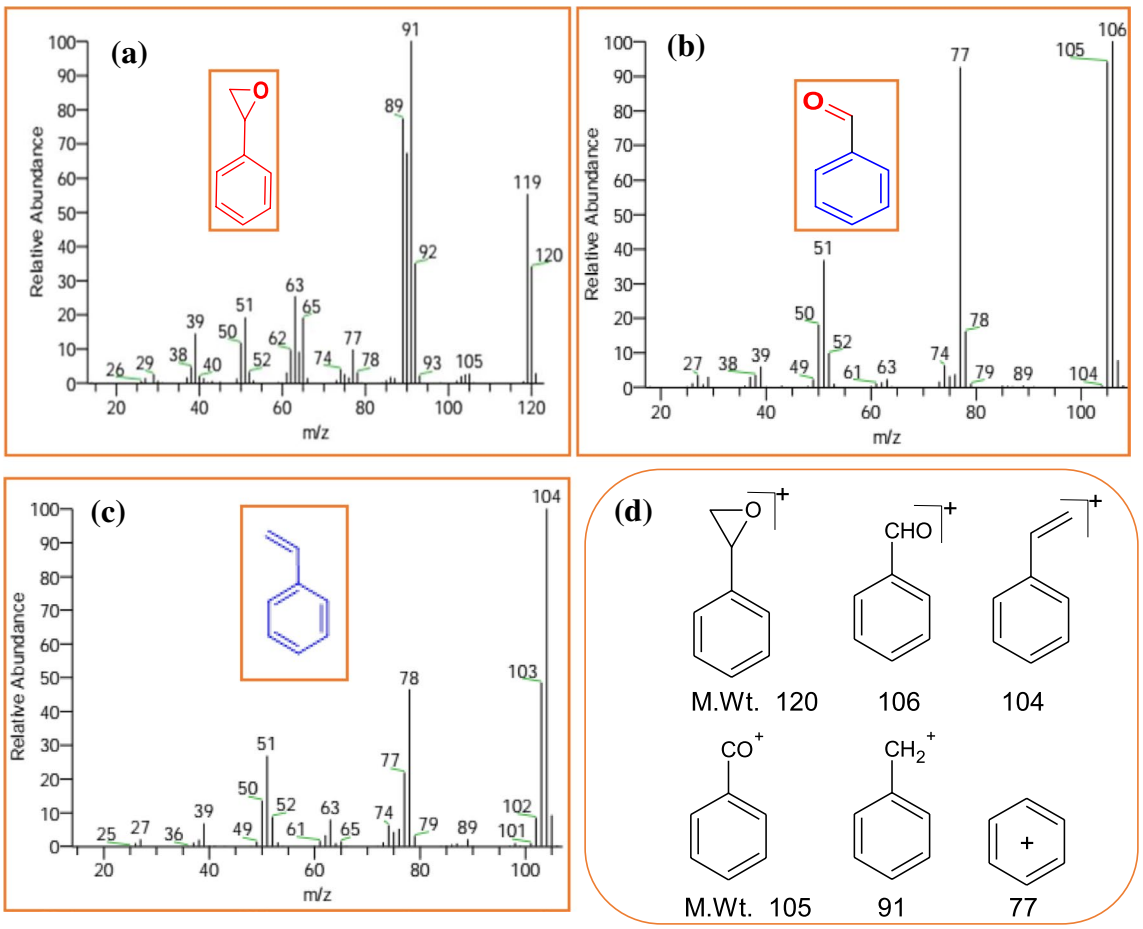


**Fig. 3** Mass spectra for the styrene oxidation using GC–MS analysis using tert-Butyl hydroperoxide

sub-stoichiometric amounts of TBHP, and molecular oxygen. Moreover, a decrease in reaction temperature decreased the yield of benzaldehyde. The amount of catalyst was fixed (0.08 mol.%, based on metal sites) compared to the literature data. $Cu_3(BTC)_2$-MOF (BTC refers to benzene-1,4,5-tricarboxylic acid) and TEMPO as oxidants offered a conversion of 62% for cinnamaldehyde [2]. However, the reaction time was long, and the amount of catalyst was three times that of the present study. In contrast, Ce-MOF exhibits high conversion in a short reaction time. It can effectively catalyze alcohol oxidation without the need for ternary metal sites such as Au@Zn/Ni-MOF-2 [44].

The mechanism for alcohol oxidation is investigated (Fig. 4a). Based on the XPS spectrum (Fig. 1**d**), Ce-MOF contains two valences of Ce ions, i.e. $Ce^{3+}$ and $Ce^{4+}$. The presence of these oxidation states ensures the Fenton-like properties. Ce-MOF can catalytically degrade hydrogen peroxide into reactive oxygen species. The fluorescence emission spectra of terephthalic acid (TPA) and hydrogen peroxide with and without Ce-MOF were measured (Fig. 4b). TPA is a non-emitted molecule. The hydroxyl derivative of TPA is an active fluorescence molecule [45, 46]. The fluorescence emission of TPA and $H_2O_2$ in the absence of Ce-MOF showed no emission (Fig. 4b). On the other side, in the presence of Ce-MOF, TPA showed emissions indicating hydroxylation. This observation suggests the formation of reactive hydroxyl species.

Ce-MOF displays several merits, including a high conversion rate and good selectivity toward styrene's epoxidation. It can be used to oxidize olefins and primary or secondary alcohol effectively. It can be reused several times, maintaining high catalytic activity (Fig. 4c). Cerium-based catalysts are effective materials for alcohol oxidation. Several cerium-based nanocatalysts were reported, including Au-$CeO_2$@SBA-15 catalysts [47] and Au\$CeO_2$ [33]. Ce-MOF is expected to support catalysts such as gold nanoparticles that enable effective catalytic oxidation of alcohol [33].

## Adsorption and Catalytic Degradation of Dyes

Ce-MOF was investigated for dye adsorption and oxidation using MeB, DB, Rh6G, and CR (Figure S1). The oxidation of the dye was monitored by measuring the UV–Vis spectra of the dyes (Fig. 5). There is an insignificant decrease in the signals recorded in UV–Vis absorption spectra of the dye in the presence of $H_2O_2$. This observation indicates that the dyes were barely degraded using $H_2O_2$ only, i.e. no catalyst such as Ce-MOF (Fig. 5). In contrast, the UV–Vis absorption peak showed a significant drop in the presence of Ce-MOF (Fig. 5). The reduction in the UV–Vis absorption of the dye reveals that Ce-MOF can be used to remove the organic dye via adsorption.

The adsorption of organic dyes using Ce-MOF is evaluated in Fig. 6a. Ce-MOF was tested for the adsorption

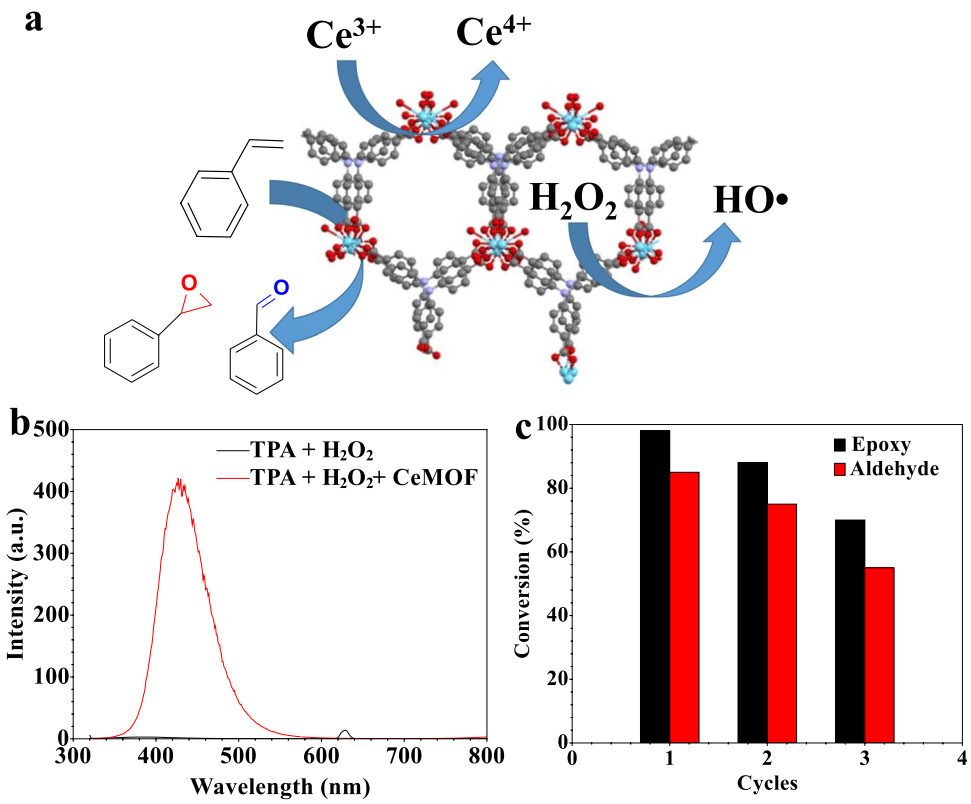


**Fig. 4** **a** mechanism for oxidation, **b** fluorescence for TPA and hydrogen peroxide with and without Ce-MOF, and **c** recyclability for styrene oxidation

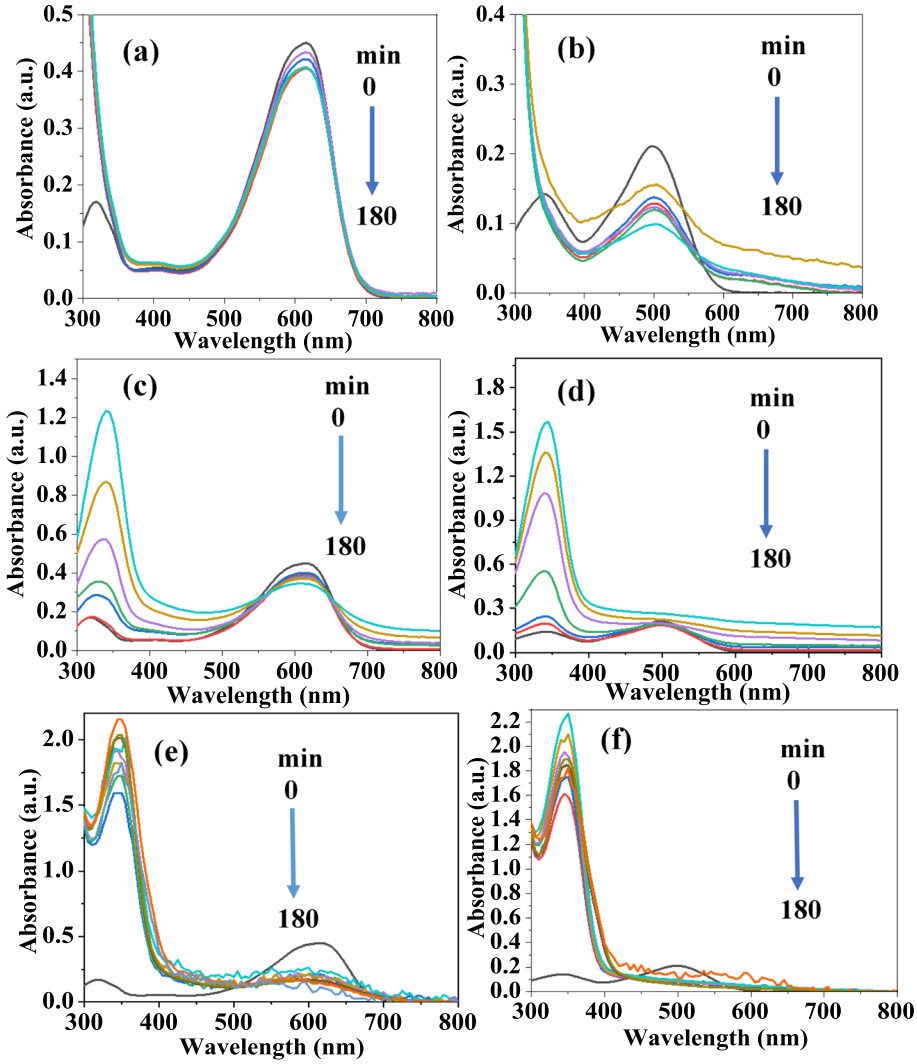


**Fig. 5** UV–Vis absorption spectra of **a**, **c**, **e** Congo red, and **b**, **d**, **f** Direct blue, **a**-**b** without catalyst in the presence of $H_2O_2$, **c**-**d** using only Ce-MOF, and **e**–**f** using Ce-MOF and $H_2O_2$

of organic dyes. It shows adsorption efficiencies of 20%, 45%, 70%, and 85% for Rh6G, CR, DR, and MeB, respectively (Fig. 6a). The dye adsorption can be achieved briefly (Fig. 6a). However, the adsorption requires a high amount of the adsorbent and a place for the material's storage after adsorption. These requirements render the dye's removal via adsorption problematic for large-scale applications. In contrast, removing the dye via degradation may be promising compared to adsorption.

The oxidation of the dye was evaluated using $H_2O_2$ in the presence and absence of Ce-MOF (Fig. 6). The oxidation efficiencies of DB and CR using $H_2O_2$ are extremely low, as

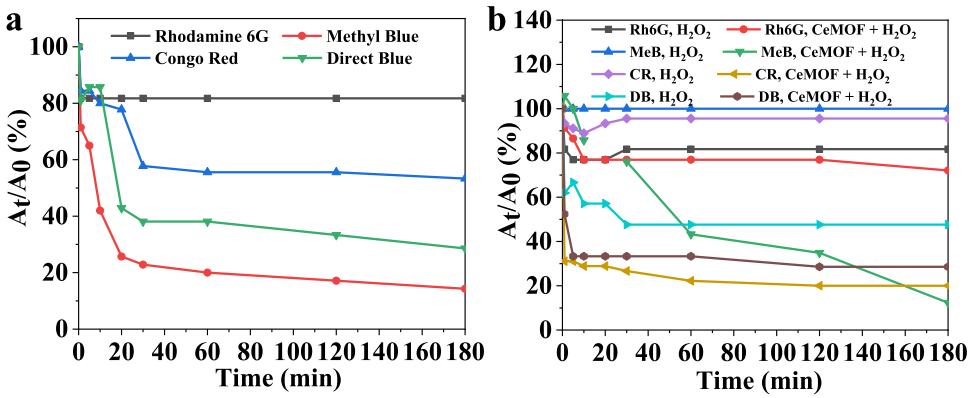


**Fig. 6** Dye removal via **a** adsorption onto Ce-MOF and **b** oxidation using $H_2O_2$ and $H_2O_2$ with Ce-MOF

shown in Fig. 6**b**. The dye oxidation using $H_2O_2$ only leads to efficiencies of 20%, < 5%, 5%, and 50% for Rh6G, MeB, CR, and DB, respectively (Fig. 6b). In contrast, $H_2O_2$ in the presence of Ce-MOF shows removal efficiencies of 30%, 90%, 80%, and 70% for Rh6G, MeB, CR, and DB, respectively, via catalysis (Fig. 6b).

The dye removal via adsorption and catalytic oxidation can be visualized via the naked eye after 180 min (Fig. 7). The color of the dye's solutions almost disappeared, indicating adsorption and catalytic oxidation. The dye can be precipitated after the adsorption and catalysis into the surface of Ce-MOF. The product can be collected via simple filtration or centrifugation (Fig. 7).

MOFs were reported as adsorbents or catalysts for the removal of organic dye removal via adsorption and degradation (Table 2). The degradability of DB and CR can be achieved entirely within a short reaction time. Compared to other MOFs, Ce-MOF offers the advantage of having a high degradation efficiency within a short time using a low material dosage (10 mg, 180 min). Dye degradation via photocatalysis using ZnO@ZIF-8 consumed high energy (UV light, high-pressure Hg lamp). Ce-MOF exhibits high removal efficiencies using low dosage compared to other photocatalysts such as NNU-15 that require six times more amount compared to Ce-MOF. MOF-589, was investigated for catalytic degradation of MB dye using $H_2O_2$ as an oxidant [32]. The authors observed no catalytic activity for iron-based heterogeneous catalysts and cerium salts (e.g., $Ce(NO_3)_3 \bullet 6H_2O$ or $CeCl_3$) [32]. Ce-doped UiO-67 was tested for the oxidation of methylene blue. It offered a removal rate of 94.1% in 30 min [48]. $NH_2$-MIL-88B(Fe) exhibited a peroxidase-like activity for the degradation of MB in an aqueous solution

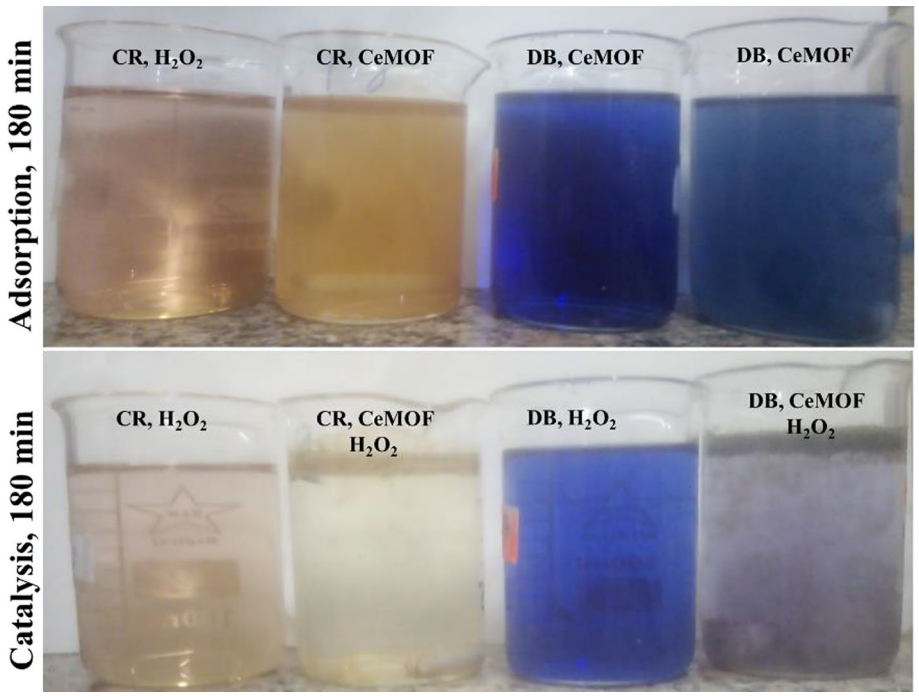


**Fig. 7** Camera image for CR and DB in the presence of $H_2O_2$ and Ce-MOF for adsorption and catalysis

**Table 2** Examples of MOF that were used as a Fenton or Photo-Fenton process for the degradation of the organic dye

| MOFs | Dye | Conditions | Efficiency | t (min) | Ref |
|---|---|---|---|---|---|
| MOF-589 | MB | Catalyst (1 mg), MB solution (20 ppm and 40 ppm, 1 mL), $H_2O_2$ (20 µL), RT | 98% | 15 | [32] |
| Ce-doped UiO-67 | MB | Catalyst (1 g $L^{-1}$), MB solution (500 ppm), $H_2O_2$ (7 mmol$L^{-1}$), at RT, pH 3 | 94.1% | 30 | [48] |
| NH2-MIL-88B(Fe) | MB | Catalyst (0.2 g $L^{-1}$), MB solution (20 mg$L^{-1}$), $H_2O_2$ (7 mmol $L^{-1}$), RT, pH 3 | 100% | 45 | [49] |
| BiOCl/MIL-100(Fe) | RhB | [Cat] = 80 mg, [Dye] = 40 mg$L^{-1}$, [$H_2O_2$] = 7.4 mmol $L^{-1}$, pH = 6.8, T = 303 K, t = 60 min, visible light (LSH-500 W xenon lamp) | 90% | 20 | [50] |
| Ce-MOF | Rh6G,<br>MeB,<br>CR,<br>DB | [Cat] = 10 mg, [Dye] = 1000 mg $L^{-1}$, [$H_2O_2$] = 5 mL $H_2O_2$(30 wt.%) | 30%<br>90%<br>80%<br>70% | 180 | Here |

Rhodamine B, RhB; Room Temperature, RT

[49]. It offered a complete degradation efficiency (100%) in 45 min using 0.2 g $L^{-1}$ of the dye concentration [49]. Lu et al. used HKUST-1/$Fe_3O_4$/CMF for the degradation of MB. They observed a degradation efficiency of 98% for MB after 4 h using 10 mg $L^{-1}$ of MB (150 mL) and 50 mg of the catalyst [36]. Ce-MOF can be used directly as the catalyst for dye degradation without the need for nanoparticles or light radiation [50]. Materials such as BiOCl and MIL-100(Fe) showed dye removal efficiencies of 10% and 20%, respectively, without light radiation in the presence of $H_2O_2$ [50].

## Conclusion

Solvothermal synthesis of Ce-MOF was achieved using cerium and a tritopic linker. The prepared Ce-MOF exhibits good crystallinity with oxidative catalytic properties. Ce-MOF can be used for the oxidation reaction of olefins, alcohol, and dyes. Olefins oxidation using styrene as a model showed conversion > 95% with excellent selectivity toward styrene epoxide over benzaldehyde. The catalytic oxidation of alcohol using Ce-MOF/$H_2O_2$ exhibited complete transformation. Ce-MOF/$H_2O_2$ removed 90% of the initial color of the dye after 180 min in a batch reaction at room temperature. Cerium-based MOF is promising for further exploration as a Fenton-like catalyst.

**Supplementary Information** The online version contains supplementary material available at https://doi.org/10.1007/s10876-022-02402-7.

**Funding** Open access funding provided by The Science, Technology & Innovation Funding Authority (STDF) in cooperation with The Egyptian Knowledge Bank (EKB).

**Data Availability** The data are available upon reasonable request.



## References

1. Z. Ma and F. Zaera, in *Encyclopedia of Inorganic Chemistry*, John Wiley & Sons Ltd, Chichester UK, 2006.
2. B. Wang, Z. Song, and L. Sun (2021). *Chem. Eng. J.* **409**.
3. X. Yue, N. L. Ma, C. Sonne, R. Guan, S. S. Lam, Q. Van Le, X. Chen, Y. Yang, H. Gu, J. Rinklebe, and W. Peng (2021). *J. Hazard. Mater.* **405**.
4. C. He, J. Cheng, X. Zhang, M. Douthwaite, S. Pattisson, and Z. Hao (2019). *Chem. Rev.* **119**, 4471–4568.
5. M. S. Kamal, S. A. Razzak, and M. M. Hossain (2016). *Atmos. Environ.* **140**, 117–134.
6. H. Huang, Y. Xu, Q. Feng, and D. Y. C. Leung (2015). Catal. *Sci. Technol.* **5**, 2649–2669.
7. Y. Guo, M. Wen, G. Li, and T. An (2021). *Appl. Catal. B Environ.* **281**.
8. Y. Ren, Y. Ma, G. Min, W. Zhang, L. Lv, and W. Zhang (2021). *Sci. Total Environ.* **762**.
9. Y. Fu, Z. Yin, L. Qin, D. Huang, H. Yi, X. Liu, S. Liu, M. Zhang, B. Li, L. Li, W. Wang, X. Zhou, Y. Li, G. Zeng, and C. Lai (2022). *J. Hazard. Mater.* **422**.
10. N. Wang, T. Zheng, G. Zhang, and P. Wang (2016). *J. Environ. Chem. Eng.* **4**, 762–787.
11. J. H. Kluytmans, A. Markusse, B. F. Kuster, G. Marin, and J. Schouten (2000). *Catal. Today* **57**, 143–155.
12. M. Pagliaro, S. Campestrini, and R. Ciriminna (2005). *Chem. Soc. Rev.* **34**, 837.
13. C. Parmeggiani and F. Cardona (2012). *Green Chem.* **14**, 547.
14. H. N. Abdelhamid and H.-F. Wu (2015). *Microchim. Acta* **182**, 1609–1617.
15. J. P. P. Lima, C. H. B. Tabelini, M. D. N. Ramos, and A. Aguiar (2021). Water. *Air, Soil Pollut.* **232**, 321.
16. C. I. Ezugwu, J. M. Sonawane, and R. Rosal (2022). *Sep. Purif. Technol.* **284**.
17. X. Wang, X. Zhang, Y. Zhang, Y. Wang, S.-P. Sun, W. D. Wu, and Z. Wu (2020). *J. Mater. Chem. A* **8**, 15513–15546.
18. H.-C. Zhou, J. R. Long, and O. M. Yaghi (2012). *Chem. Rev.* **112**, 673–674.
19. B. Li, M. Chrzanowski, Y. Zhang, and S. Ma (2016). *Coord. Chem. Rev.* **307**, 106–129.
20. A.Z. Kassem, H.N. Abdelhamid, D.M. Fouad, and S.A. Said (2020). *Micropor. Mesopor. Mat.* **305**, 110340.
21. A.Z. Kassem, H.N. Abdelhamid, D.M. Fouad, and S.A. Said (2021). *J. Environ. Chem. Eng.* **9**, 104401.
22. X.-M. Liu, L.-H. Xie, and Y. Wu (2020). *Inorg. Chem. Front.* **7**, 2840–2866.
23. H.N. Abdelhamid and A. Mathew (2022). *Coord. Chem. Rev.* **451**, 214263.
24. S. Sultan, H. N. Abdelhamid, X. Zou and A. P. Mathew, *Adv. Funct. Mater.*, 2018, 1805372.
25. H. N. Abdelhamid, M. Wilk-Kozubek, A. M. El-Zohry, A. Bermejo Gómez, A. Valiente, B. Martín-Matute, A.-V. A.-V. Mudring and X. Zou, *Microporous Mesoporous Mater.*, 2019, **279**, 400–406.
26. H.N. Abdelhamid (2021). *J. Environ. Chem. Eng.* **9**, 104404.
27. H.N. Abdelhamid and W. Sharmoukh (2021). *Microchem. J.* **163**, 105873.
28. H. N. Abdelhamid, G.A.-E. Mahmoud, and W. Sharmouk (2020). *J. Mater. Chem. B* **8**, 7548–7556.
29. R. M. Rego, G. Kuriya, M. D. Kurkuri, and M. Kigga (2020). *J. Hazard. Mater.* **403**, 123605.
30. Q. Wu, H. Yang, L. Kang, Z. Gao, and F. Ren (2020). *Appl. Catal. B Environ.* **263**.
31. J. Jacobsen, A. Ienco, R. D'Amato, F. Costantino, and N. Stock (2020). The chemistry of Ce-based metal–organic frameworks. *Dalt Trans*. https://doi.org/10.1039/D0DT02813D.
32. G. H. Dang, Y. B. N. Tran, T. V. Pham, V. T. Pham, N. T. H. Luu, H. D. Nguyen, P. T. K. Nguyen, H. T. D. Nguyen, and T. Truong (2019). *Chempluschem* **84**, 1046–1051.
33. A. Abad, P. Concepción, A. Corma, and H. García (2005). *Angew. Chemie Int. Ed.* **44**, 4066–4069.

34. Q. Yao, A. Bermejo Gómez, J. Su, V. Pascanu, Y. Yun, H. Zheng, H. Chen, L. Liu, H. N. Abdelhamid, B. Martín-Matute, and X. Zou (2015). Series of highly stable isoreticular lanthanide metal-organic frameworks with expanding pore size and tunable luminescent properties. *Chem. Mater.* **27**, 5332–5339.
35. K. H. Hussein, H. N. Abdelhamid, X. Zou, and H.-M. Woo (2019). *Mater. Sci. Eng. C* **94**, 484–492.
36. H. N. Abdelhamid, A. Talib, and H. F. Wu (2017). *Talanta* **166**, 357–363.
37. H. N. Abdelhamid and H.-F. Wu (2014). *J. Am. Soc. Mass Spectrom.* **25**, 861–868.
38. H. N. Abdelhamid, J. Gopal, and H.-F.F. Wu (2013). *Anal. Chim. Acta* **767**, 104–111.
39. Q. Yao, A. B. Gómez, J. Su, V. Pascanu, Y. Yun, H. Zheng, H. Chen, L. Liu, H. N. Abdelhamid, B. Martín-Matute, and X. Zou (2015). *Chem. Mater.* **27**, 5332–5339.
40. H. E. Emam, H. N. Abdelhamid, and R. M. Abdelhameed (2018). *Dye. Pigment.* **159**, 491–498.
41. E. Bêche, P. Charvin, D. Perarnau, S. Abanades, and G. Flamant (2008). *Surf. Interface Anal.* **40**, 264–267.
42. K. I. Maslakov, Y. A. Teterin, A. J. Popel, A. Y. Teterin, K. E. Ivanov, S. N. Kalmykov, V. G. Petrov, P. K. Petrov, and I. Farnan (2018). *Appl. Surf. Sci.* **448**, 154–162.
43. X. Zou, Q. Yao, A. B. Gómez, J. Su, V. Pascanu, Y. Yun, H. Zheng, H. Chen, L. Liu, H. N. Abdelhamid, and B. Martín-Matute (2016). *Acta Crystallogr. Sect. A Found. Adv.* **72**, s136–s136.
44. N. Qin, A. Pan, J. Yuan, F. Ke, X. Wu, J. Zhu, J. Liu, J. Zhu, and A. C. S. Appl (2021). *Mater. Interfaces* **13**, 12463–12471.
45. A. I. A. Soliman, A.-M.A. Abdel-Wahab, and H. N. Abdelhamid (2022). *RSC Adv.* **12**, 7075–7084.
46. A. I. A. Soliman, H. N. Abdelhamid and Aboel-Magd A. Abdel-Wahab, *ChemRxiv. Cambridge Cambridge Open Engag. 2022;*, 2022, https://doi.org/10.26434/chemrxiv-2022-rwvtp.
47. T. Wang, X. Yuan, S. Li, L. Zeng, and J. Gong (2015). *Nanoscale* **7**, 7593–7602.
48. X. Dong, Y. Lin, G. Ren, Y. Ma, and L. Zhao (2021). *Colloids Surfaces A Physicochem. Eng. Asp.* **608**.
49. J. He, Y. Zhang, X. Zhang, and Y. Huang (2018). *Sci. Rep.* **8**, 5159.
50. D. Wu, J. Jiang, N. Tian, M. Wang, J. Huang, D. Yu, M. Wu, H. Ni, and P. Ye (2021). *RSC Adv.* **11**, 32383–32393.